# Electrosynthesized fluorinated polybithiophenes for ammonia sensing

Petr Bečvář,[a] Anna Krystianiak,[b] Sujithkumar Ganesh Moorthy,[a] Barbora Jansová,[a,c] Michal Kohout,[c] Rita Meunier-Prest,[a] and Marcel Bouvet *[a]

[a.] *Institut de Chimie Moléculaire de l'Université de Bourgogne, UMR CNRS 6302, Université de Bourgogne, 9 Avenue Alain Savary, Dijon Cedex 21078, France*
[b.] *Laboratoire Interdisciplinaire Carnot de Bourgogne (LICB), UMR CNRS 6303, Université de Bourgogne, 9 Avenue Alain Savary, Dijon Cedex 21078, France.*
[c.] *Ústav organické chemie Vysoké školy chemicko-technilogické v Praze (Department of organic chemistry, UCT Prague), Technická 5, 160 00 Praha 6-Dejvice, Czech Republic*

*Corresponding author : marcel.bouvet@u-bourgogne.fr,

**Table S1** Measured (from literature) and computed data (this work) for given group of molecules and the deviation between these data.

| | measurement | | | B3PW91/D3BJ/def2-SVP/CPCM | | | deviations | | |
|---|---|---|---|---|---|---|---|---|---|
| | HOMO | LUMO | GAP | HOMO | LUMO | GAP | HOMO | LUMO | GAP |
| α6T [THF][1] | -5.20 | **-2.65** | **2.55** | -5.16 | -2.51 | 2.65 | 0.04 | 0.14 | 0.10 |
| F4TF [THF][1] | -5.48 | **-2.85** | **2.63** | -5.42 | -2.61 | 2.80 | 0.06 | 0.24 | 0.17 |
| 2[d] [THF][1] | -5.64 | **-2.82** | **2.82** | -5.71 | -2.73 | 2.98 | -0.07 | 0.09 | 0.16 |
| 3[e] [THF][1] | -5.81 | **-2.81** | **3.00** | -5.81 | -2.51 | 3.30 | 0.00 | 0.30 | 0.30 |
| PE3T [DCM][2] | -5.67 | **-2.90** | **2.77** | -5.50 | -2.45 | 3.05 | 0.17 | 0.45 | 0.28 |
| PE4T [DCM][2] | -5.69 | **-2.95** | **2.74** | -5.31 | -2.51 | 2.81 | 0.38 | 0.44 | 0.07 |
| 3TEA [DCM][2] | -5.41 | **-2.75** | **2.66** | -5.15 | -2.26 | 2.89 | 0.26 | 0.50 | 0.23 |
| I2TEA [DCM][2] | -5.42 | **-2.52** | **2.90** | -5.25 | -2.10 | 3.15 | 0.17 | 0.42 | 0.25 |
| NDI-1TH [MeCN:B][3] | -6.10 | **-3.97** | **2.13** | -6.06 | -3.56 | 2.50 | 0.04 | 0.41 | 0.37 |
| NDI-2T [MeCN:B][3] | -5.80 | **-4.12** | **1.68** | -5.75 | -3.63 | 2.12 | 0.05 | 0.49 | 0.44 |
| NDI-2TH [MeCN:B][3] | -5.70 | **-4.00** | **1.70** | -5.74 | -3.63 | 2.11 | -0.04 | 0.37 | 0.41 |
| NDI-3T [MeCN:B][3] | -5.60 | **-4.14** | **1.46** | -5.49 | -3.64 | 1.85 | 0.11 | 0.50 | 0.39 |
| NDI-3TH [MeCN:B][3] | -5.50 | **-4.10** | **1.40** | -5.40 | -3.63 | 1.77 | 0.10 | 0.47 | 0.37 |
| NDI-4TH [MeCN:B][3] | -5.46 | **-4.13** | **1.33** | -5.28 | -3.64 | 1.64 | 0.18 | 0.49 | 0.31 |

[d.] 5,5'-Bis{1-[4-(thien-2-yl)-2,3,5,6-tetrafluorophenyl)]}-2,2'-dithiophene
[e.] 4,4'-Bis[5-(2,2'-dithiophenyl)]-octafluorobiphenyl

Minimal, mean and maximal values of deviations for all molecules calculated at level of theory B3PW91/D3BJ/def2-SVP/CPCM against experimental values from **Table S1**.

| Deviation | HOMO | LUMO | GAP |
|---|---|---|---|
| min | 0.00 | 0.06 | 0.07 |
| average | 0.12 | 0.36 | 0.26 |
| max | 0.38 | 0.50 | 0.44 |

Minimal, mean and maximal values of deviations from **Table S1** excluding NDI molecules. Comparison of two basis sets.

| | def2-SVP | | | ma-def2-SVP | | |
|---|---|---|---|---|---|---|
| Deviation | HOMO | LUMO | GAP | HOMO | LUMO | GAP |
| min | 0.00 | 0.09 | 0.07 | 0.04 | 0.01 | 0.02 |
| mean | 0.14 | 0.32 | 0.20 | 0.14 | 0.20 | 0.19 |
| max | 0.38 | 0.50 | 0.30 | 0.29 | 0.37 | 0.36 |

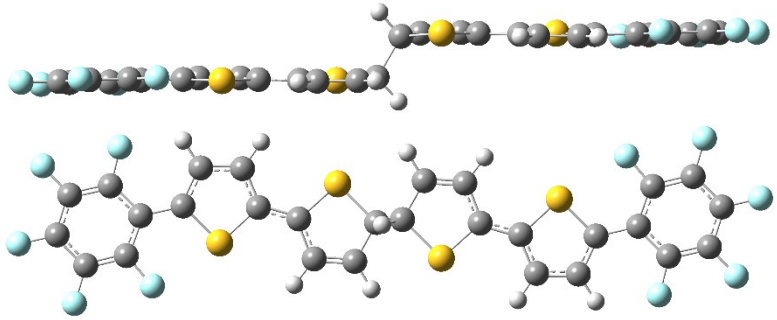

**Figure S1** $H_2F4TF^{+\cdot}$ visualized by GaussView 16.

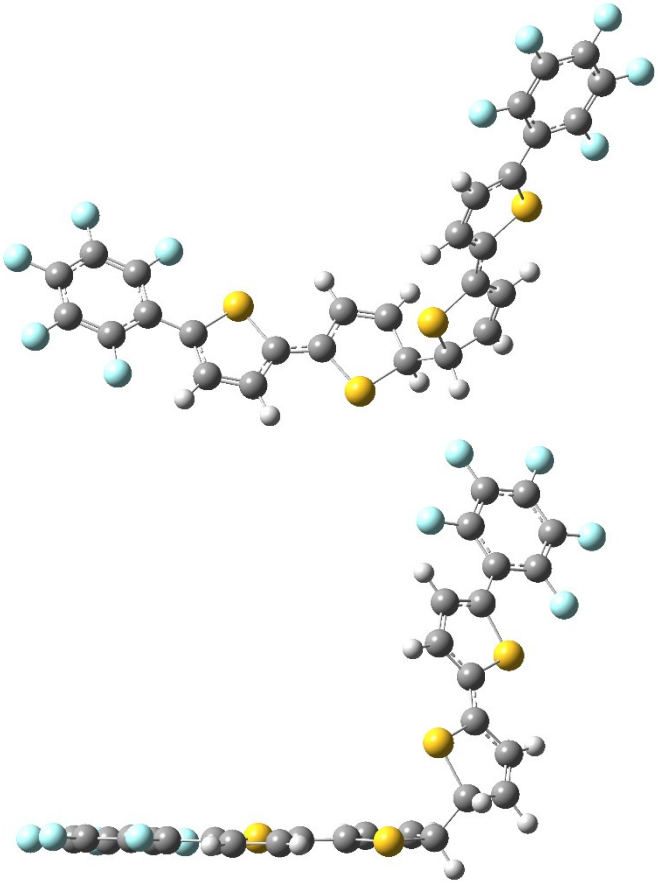

**Figure S2** $H_2F4TF^{2+}$ visualized by GaussView 16.

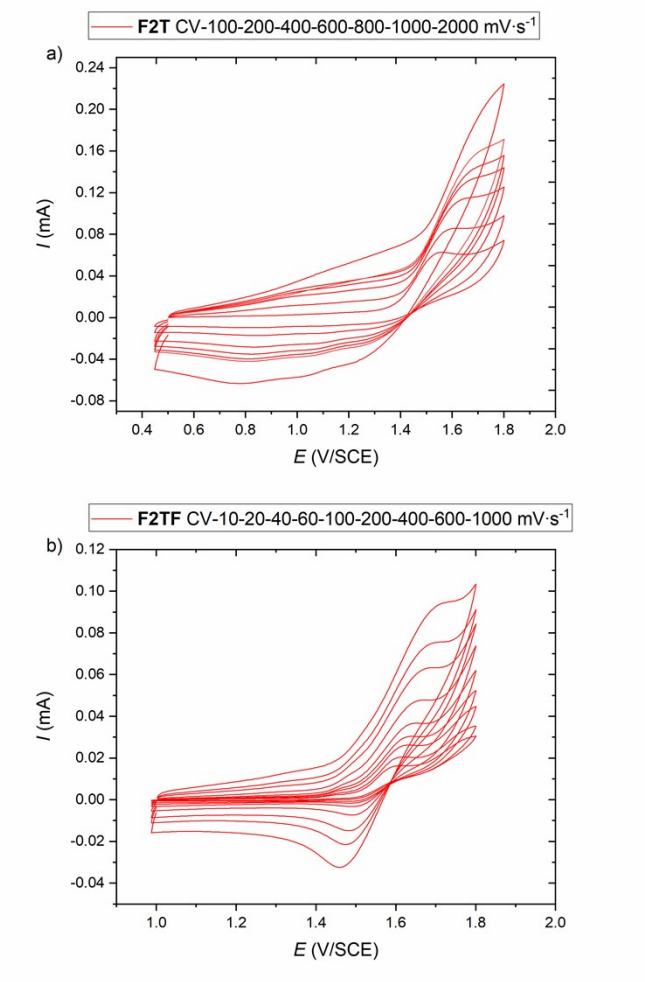


**Figure S3** CV **a)** $10^{-3}$ M of **F2T**; 3 mm C-working electrode; TBAP in $CH_2Cl_2$, 0.1 M, $v$ = 0.1; 0.2; 0.4; 0.6; 0.8; 1; 2 V·s$^{-1}$; **b)** $10^{-3}$ M of **F2TF**; 3 mm C-working electrode; TBAP in $CH_2Cl_2$, 0.1 M), $v$ = 0.01; 0.02; 0.04; 0.06; 0.1; 0.2; 0.4; 0.6; 1 V·s$^{-1}$.

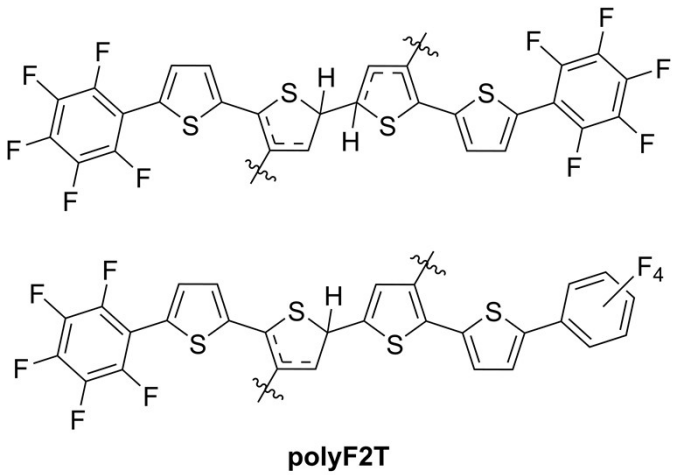


**Figure S4** Proposed structure of **polyF2T** based on two molecular unit, where the prolongation is by other monomers, formed oligomers or bithiophene. We assumed that all prepared copolymers are based on the same unites, where the prolongation is predominated by thiophene instead of **F2T** or **2T**.

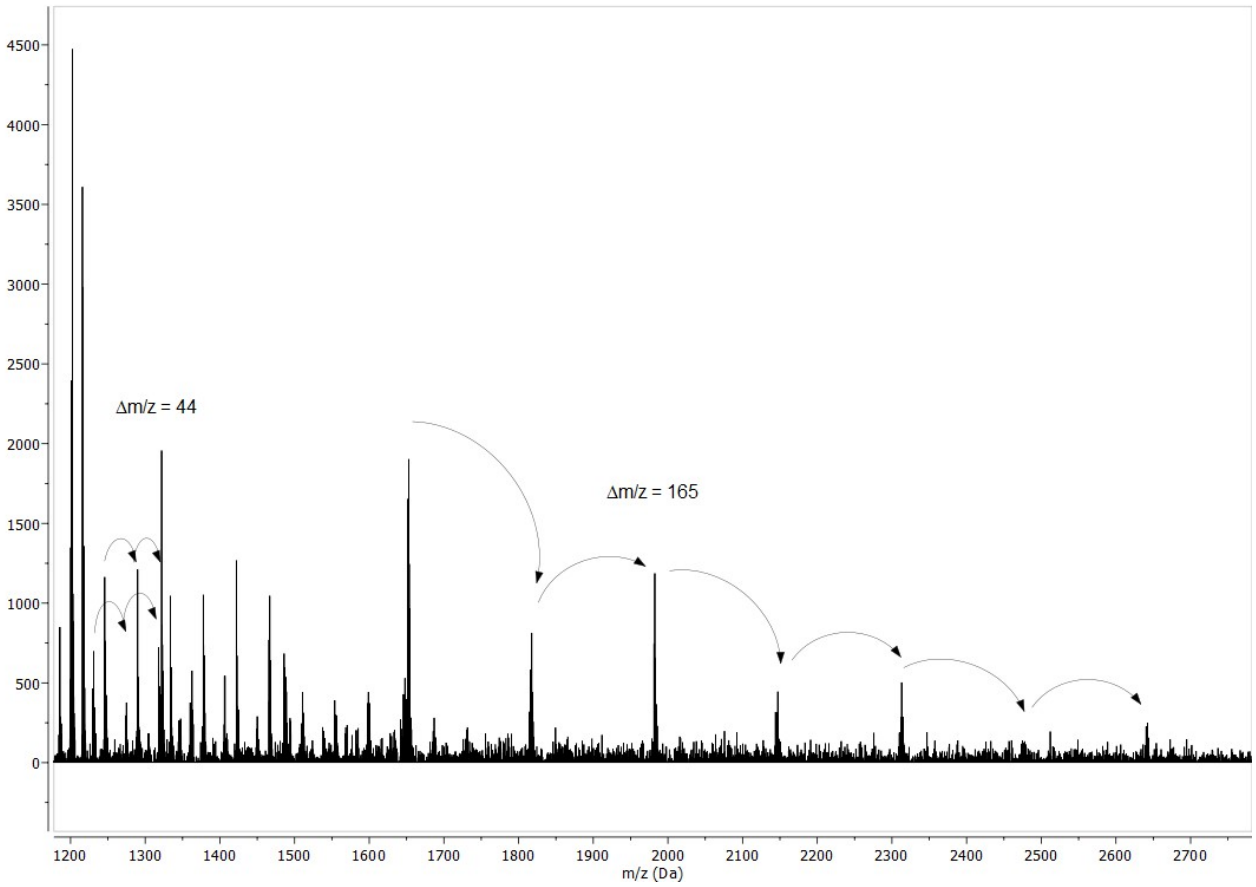


**Figure S5** Mass spectrum of oligomer mixture residue after electropolymerisation experiment of **F2T**.

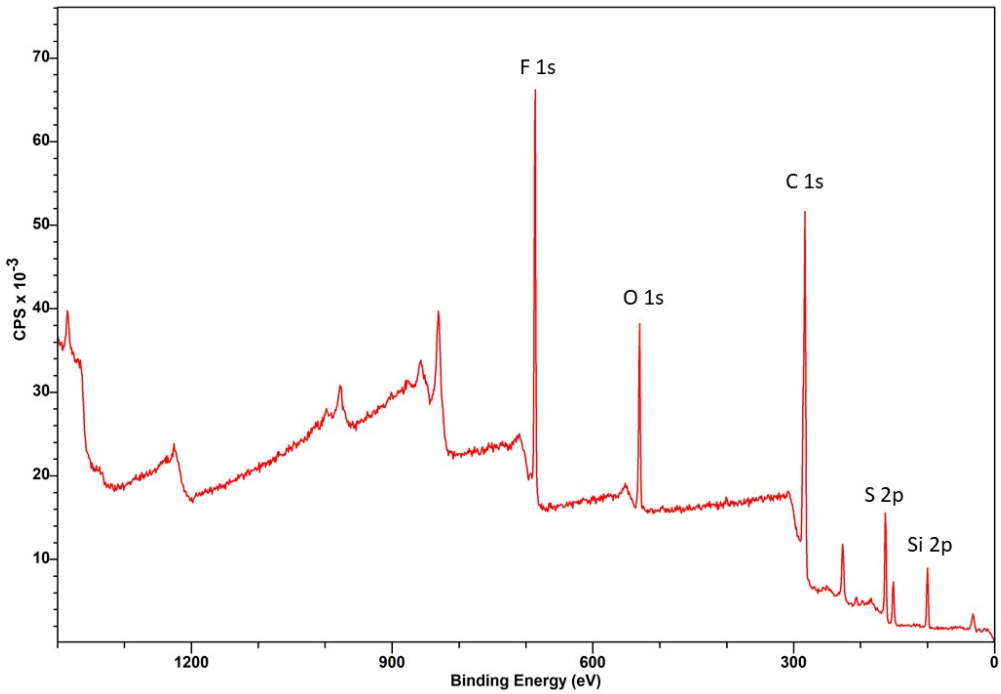


**Figure S6** XPS Survey spectrum of **polyF2T (10 scans)** covered ITO-bearing QCM quartz.

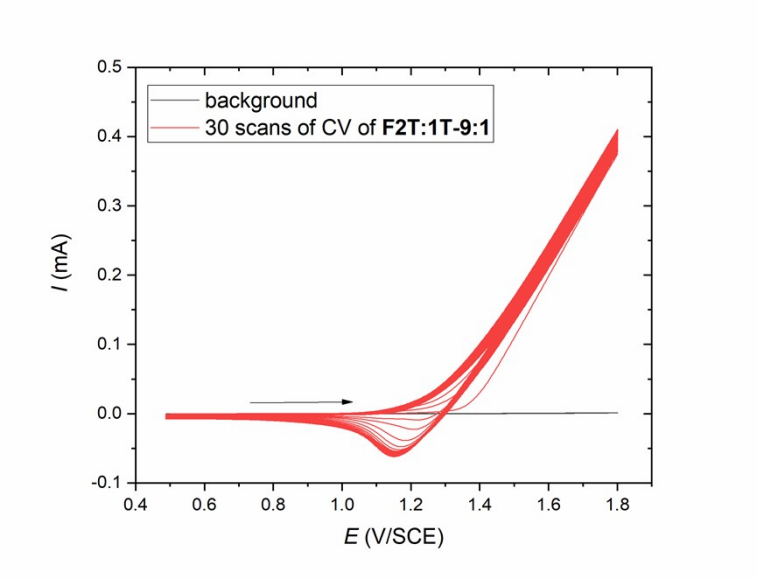


**Figure S7** 30 scans of CV (**F2T** ($0.9 \cdot 10^{-2}$ M) + **1T** ($0.1 \cdot 10^{-2}$ M); ITO-IDE as working electrode; TBAP in $CH_2Cl_2$, 0.1 M), $v$ = 0.01 V/s, $Q_{total}$ = 59.84 mC.

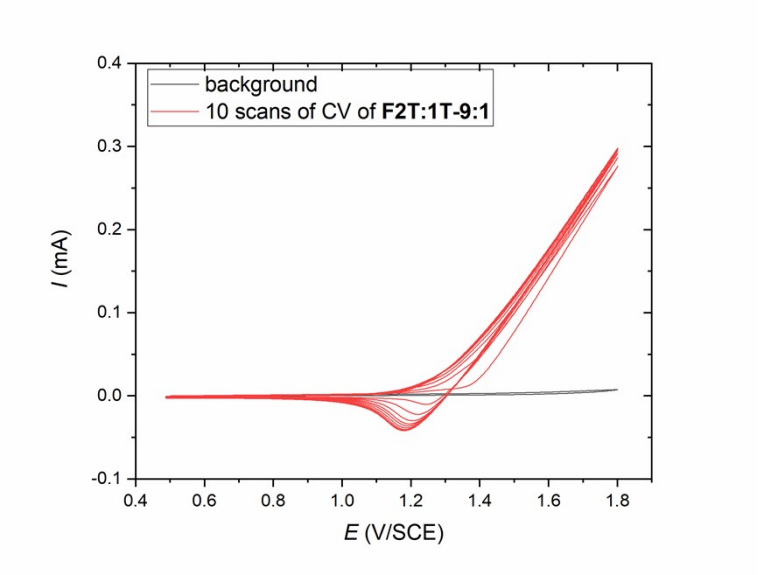


**Figure S8** 10 scans of CV (**F2T** ($0.9 \cdot 10^{-2}$ M) + **1T** ($0.1 \cdot 10^{-2}$ M); ITO-IDE as working electrode; TBAP in $CH_2Cl_2$, 0.1 M), $v$ = 0.01 V/s, $Q_{total}$ = 13.84 mC.

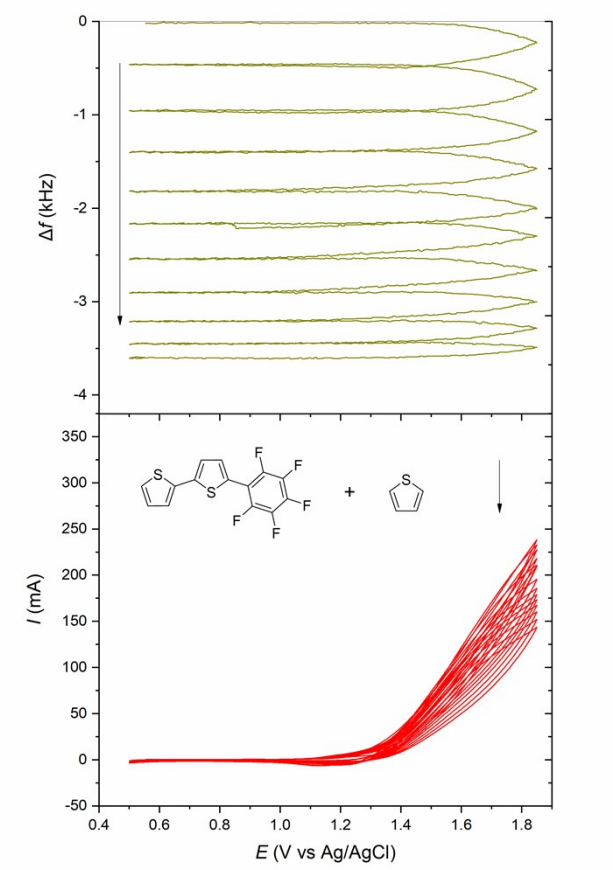


**Figure S9** Frequency change and corresponding CV of **5:5** copolymerisation experiment.

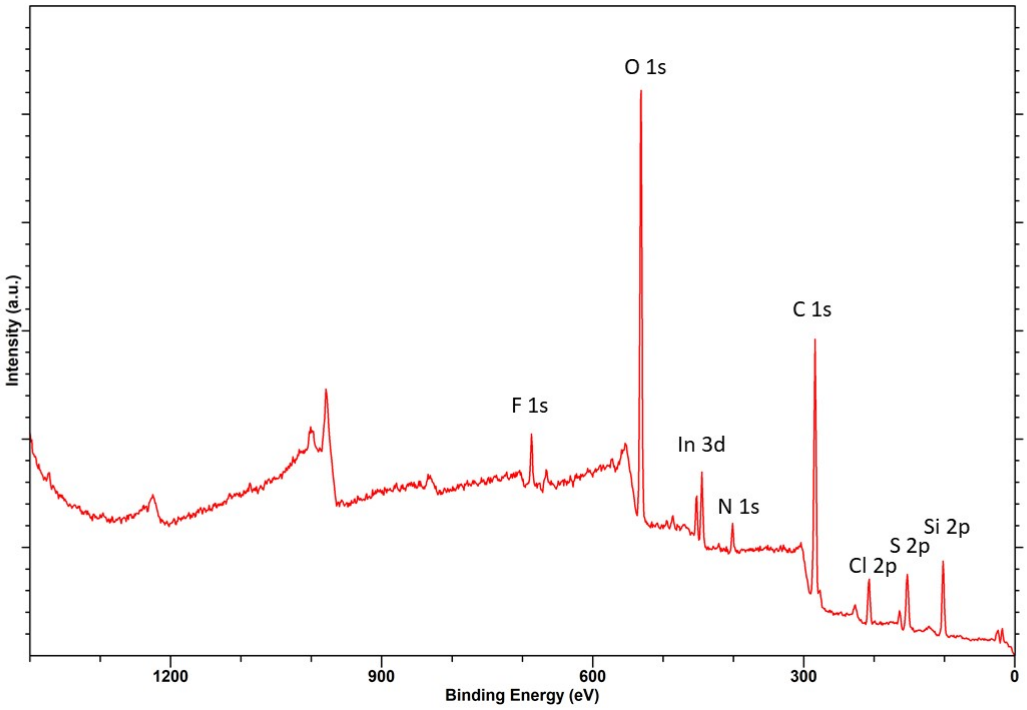


**Figure S10** XPS Survey spectrum of **copolyF2T:1T-9:1 (100 scans)** covered glass.

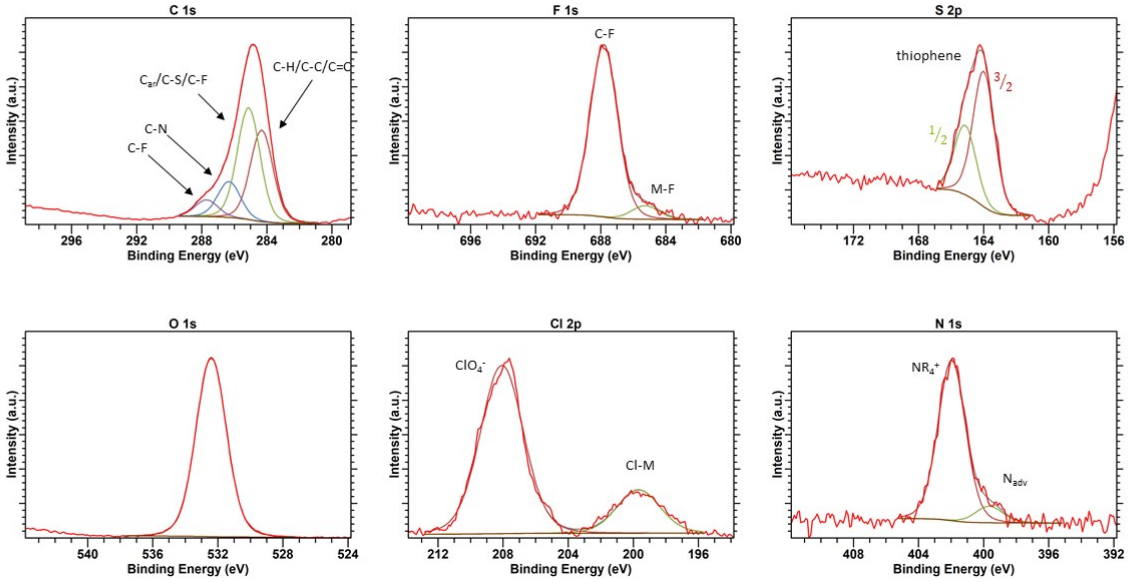


**Figure S11** XPS high resolution spectra of **copolyF2T:1T-9:1 (100 scans)** covered glass.

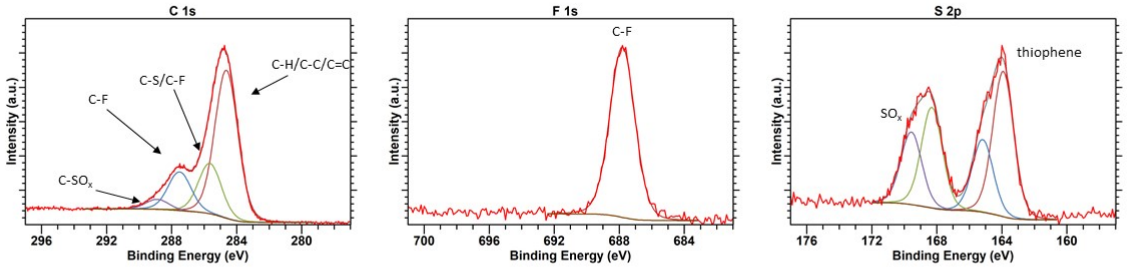


**Figure S12** XPS high resolution spectra of UV light exposed **copolyF2T:1T-5:5 (10 scans)** covered ITO IDE.

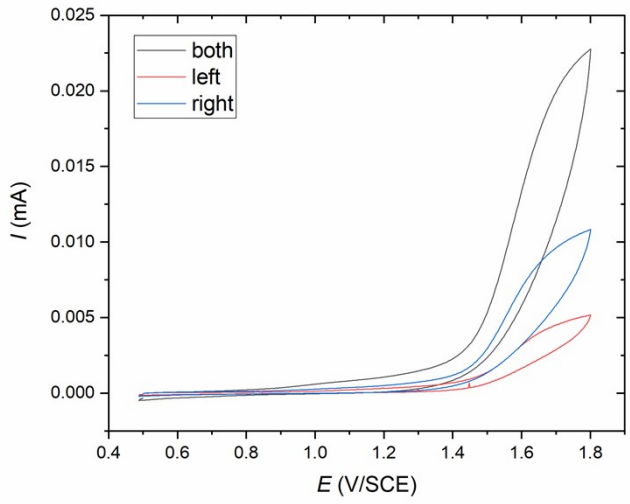


**Figure S13** CV (ITO-IDE as working electrode (**left**, **right**, **both parts**); TBAP in $CH_2Cl_2$, 0.1 M), v = 0.1 V/s

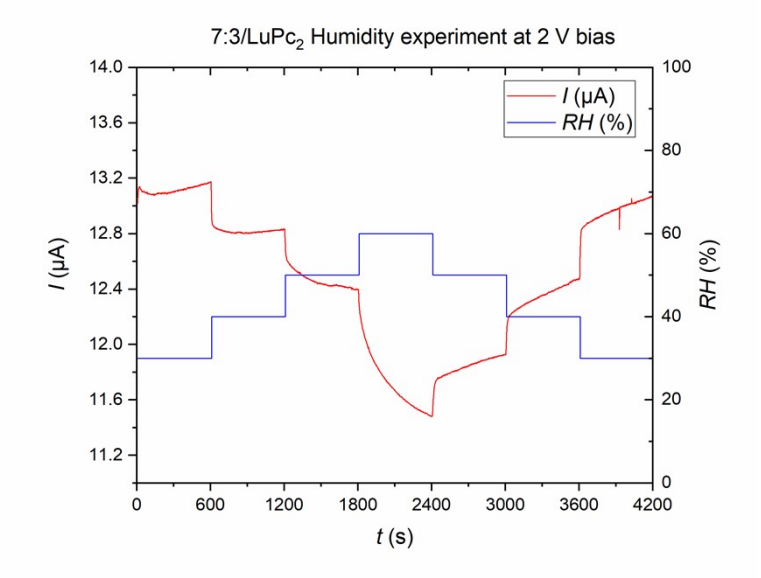


**Figure S14** Humidity experiment of 7:3/LuPc2 sensor.

**Table S2** Parameters for Langmuir equation fitting, where $y$ represents $RR$ and $x$ represents $c_{NH3}$.

| Model | LangmuirEXT1 | | | | | |
|---|---|---|---|---|---|---|
| Equation | $y = \frac{abx^{1-c}}{1+bx^{1-c}}$ | | | | | |
| Plot | **9:1** | **8:2** | **7:3** | **5:5** | **asy9:1-5:5** | **asy7:3-5:5** |
| a | -7.44 ± 0.07 | -2.71 ± 0.04 | -5.60 ± 0.05 | -12 ± 4 | -100 ± 1900 | -9.2± 1.6 |
| b | 0.1367 ± 0.0007 | 0.056 ± 0.009 | 0.1515 ± 0.0006 | 0.043 ± 0.006 | 0.01 ± 0.17 | 0.084 ± 0.010 |
| c | 0.355 ± 0.007 | -0.10 ± 0.06 | 0.418 ± 0.006 | 0.28 ± 0.12 | 0.6 ± 0.3 | 0.51 ± 0.04 |
| Reduced Chi-Sqr | 0.03804 | 0.17062 | 0.0622 | 0.96287 | 0.53643 | 0.91026 |
| R-Square (COD) | 0.99999 | 0.99935 | 0.99999 | 0.99785 | 0.99198 | 0.99957 |
| Adj. R-Square | 0.99999 | 0.99869 | 0.99999 | 0.99569 | 0.98395 | 0.99914 |

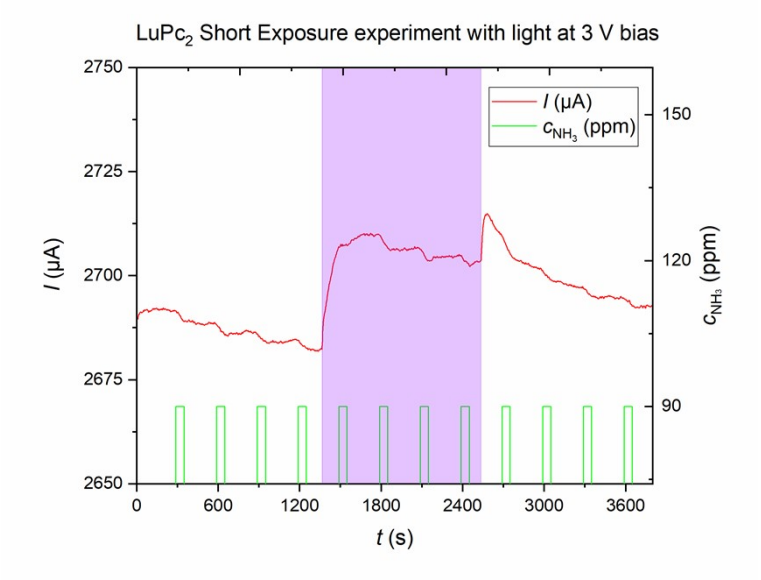


**Figure S15** Light experiment with a short exposure of 90-ppm (mol/mol) ammonia with 20% duty cycle (1 min:4 min) of $LuPc_2$ resistor; the purple areas sign periods where the UV light (365 nm) was turned on. The temperature was maintained in a range 19.6-20.4 °C. Thus, the instability of system is due to phthalocyanine decay.

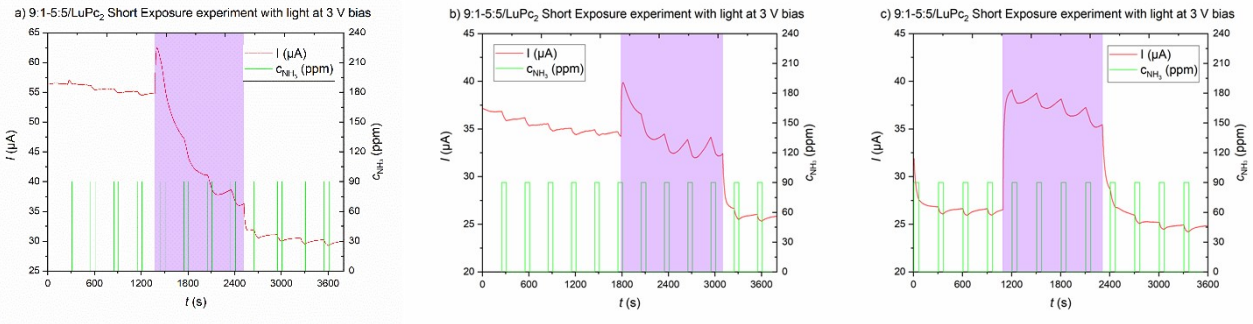


**Figure S16** Three successive light experiments with a short exposure of 90-ppm (mol/mol) ammonia with 20% duty cycle (1 min:4 min) of **asymmetric9:1-5:5**/$LuPc_2$ resistor; the purple areas sign periods where the UV light (365 nm) was turned on. The temperature was maintained in a range 19.6-20.4 °C. Its observable evolution of system during irradiation.

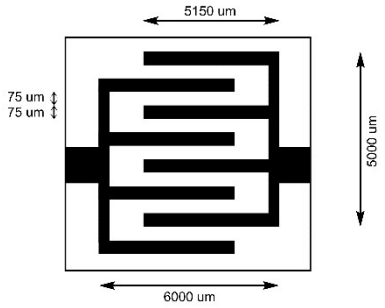


**Figure S17** Geometry of the ITO-IDE used to build heterojunction devices.

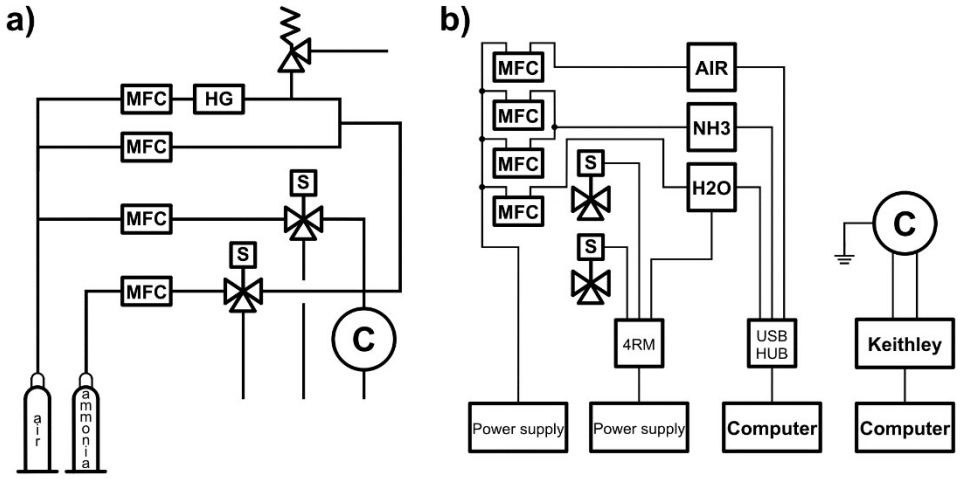


**Scheme S1** Scheme of the workstation; a) pipeline: MFC – mass flow controller, HG – humidity generator, S – solenoid three-way valve, C – sensor chamber; b) electric connection: $NH_3$, AIR, $H_2O$ – data buses (2× NI USB-6009 and, 1× NI USB-6008, respectively), 4RM – 4 Channel 5 V Relay Module (Songle; using only one relay), two 24 V Power supplies.

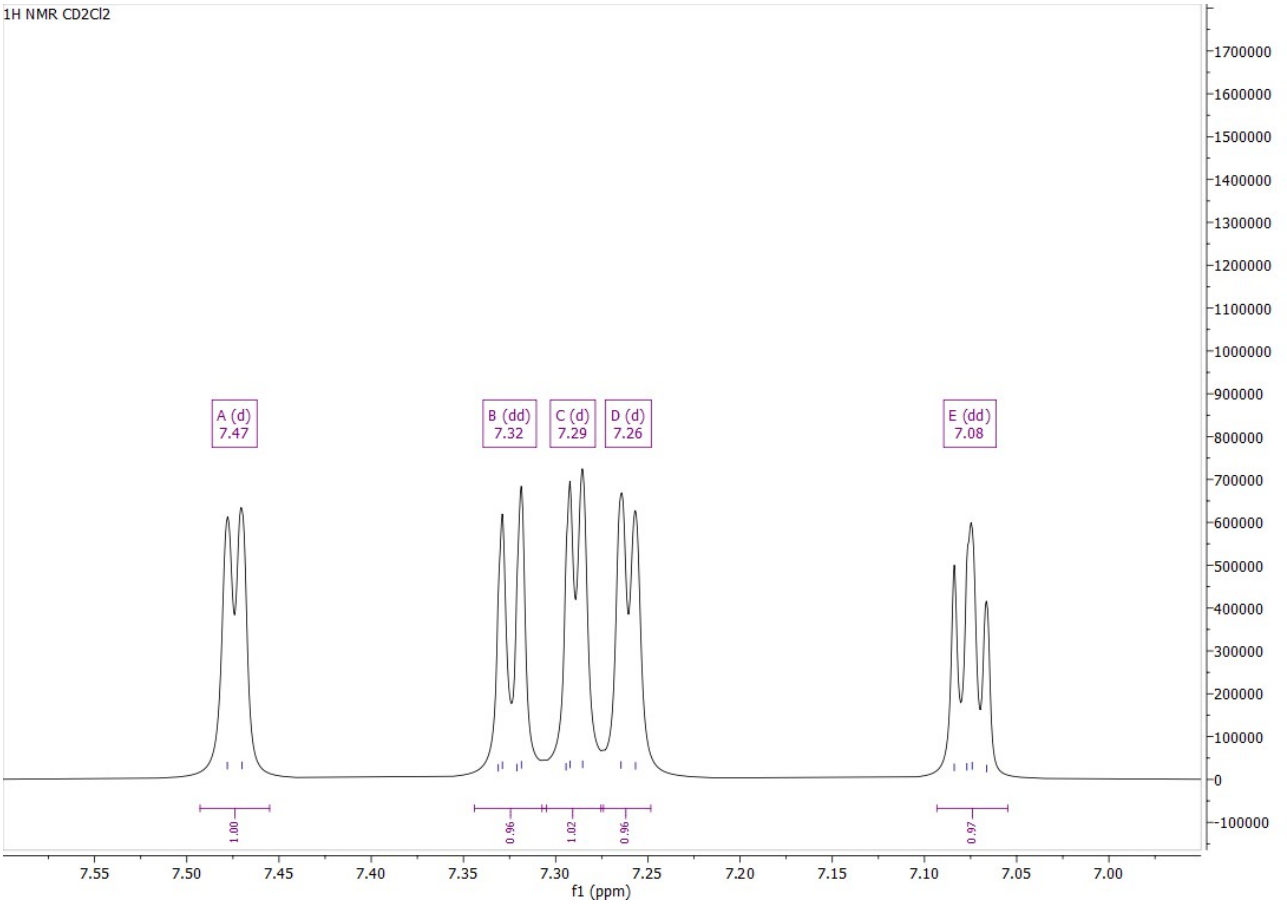


**Figure S18** $^1$H NMR of 2,2'-bithiophene in $CDCl_3$.

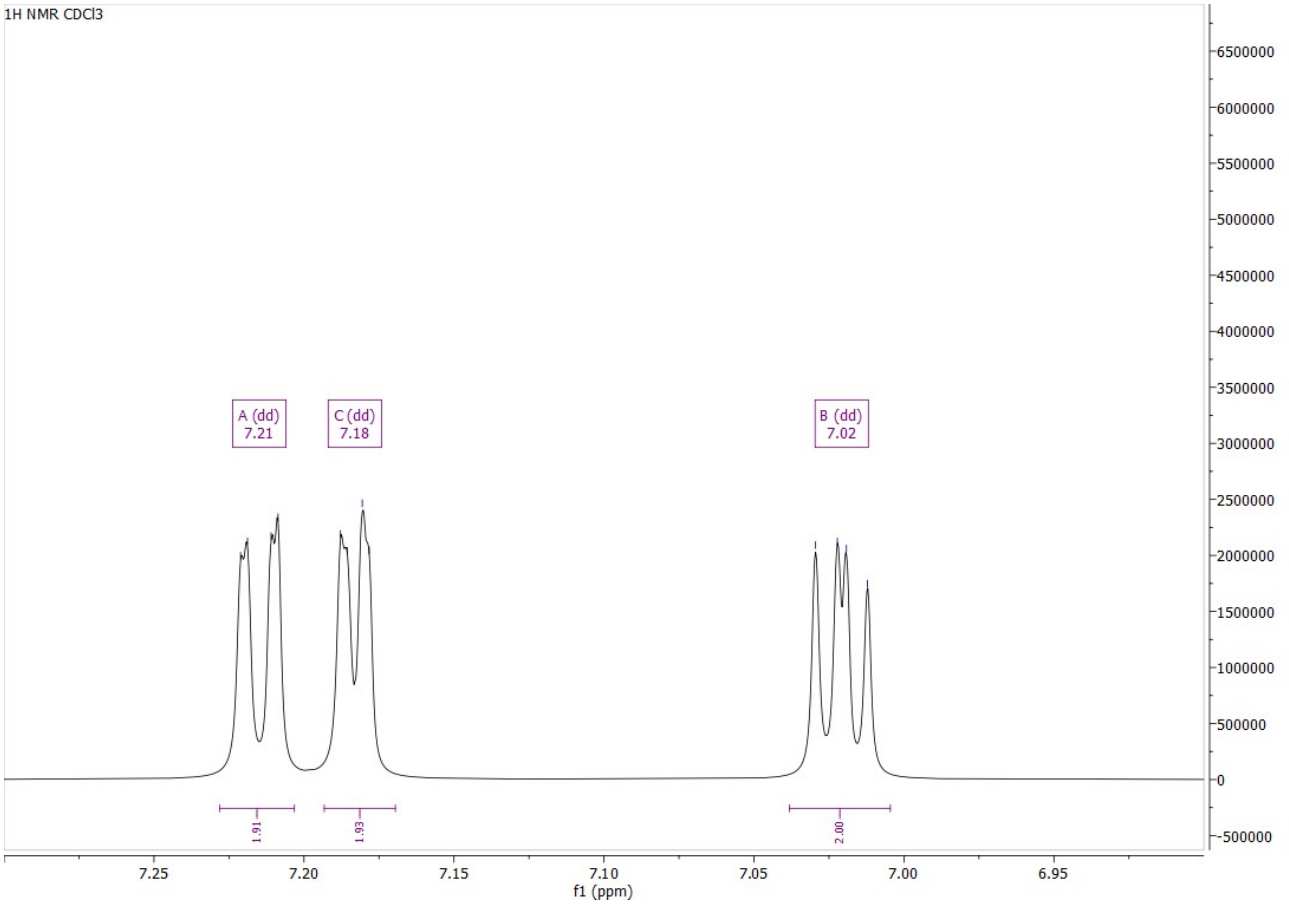


**Figure S19** $^{1}$H NMR of 5-(pentafluorophenyl)-2,2'-bithiophene in $CD_2Cl_2$.

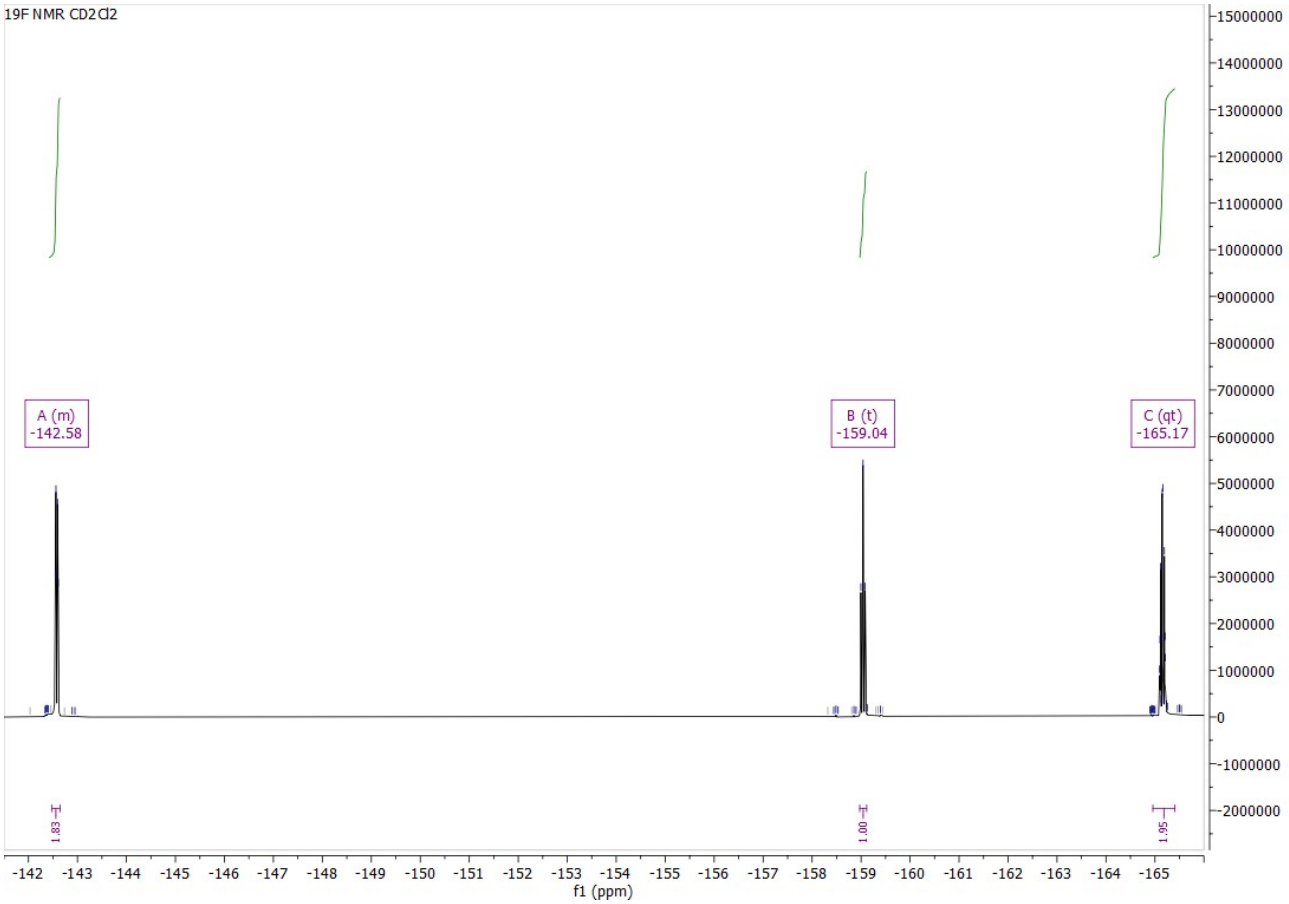


**Figure S20** $^{19}F$ NMR of 5-(pentafluorophenyl)-2,2'-bithiophene in $CD_2Cl_2$.

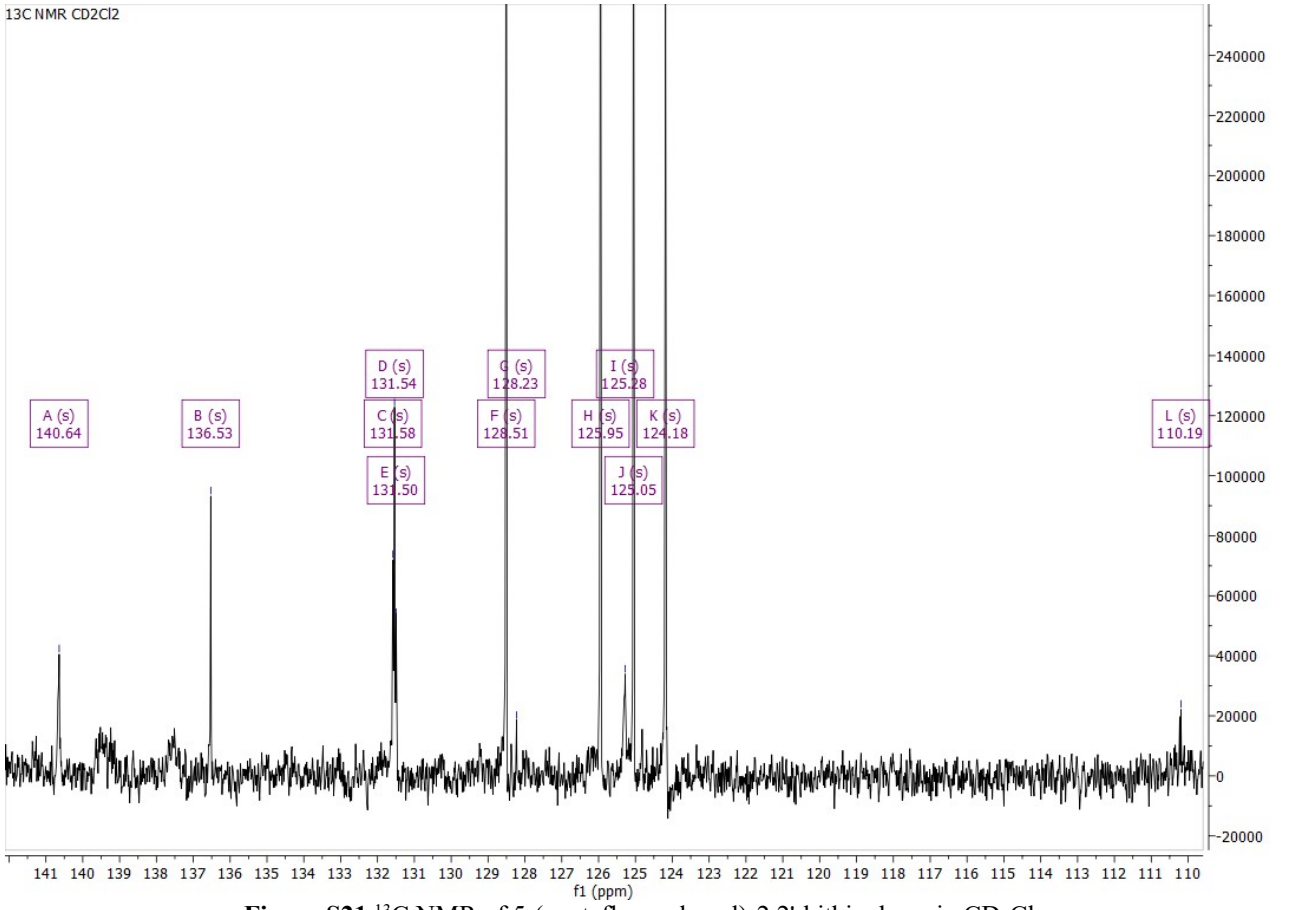


**Figure S21** $^{13}C$ NMR of 5-(pentafluorophenyl)-2,2'-bithiophene in $CD_2Cl_2$.

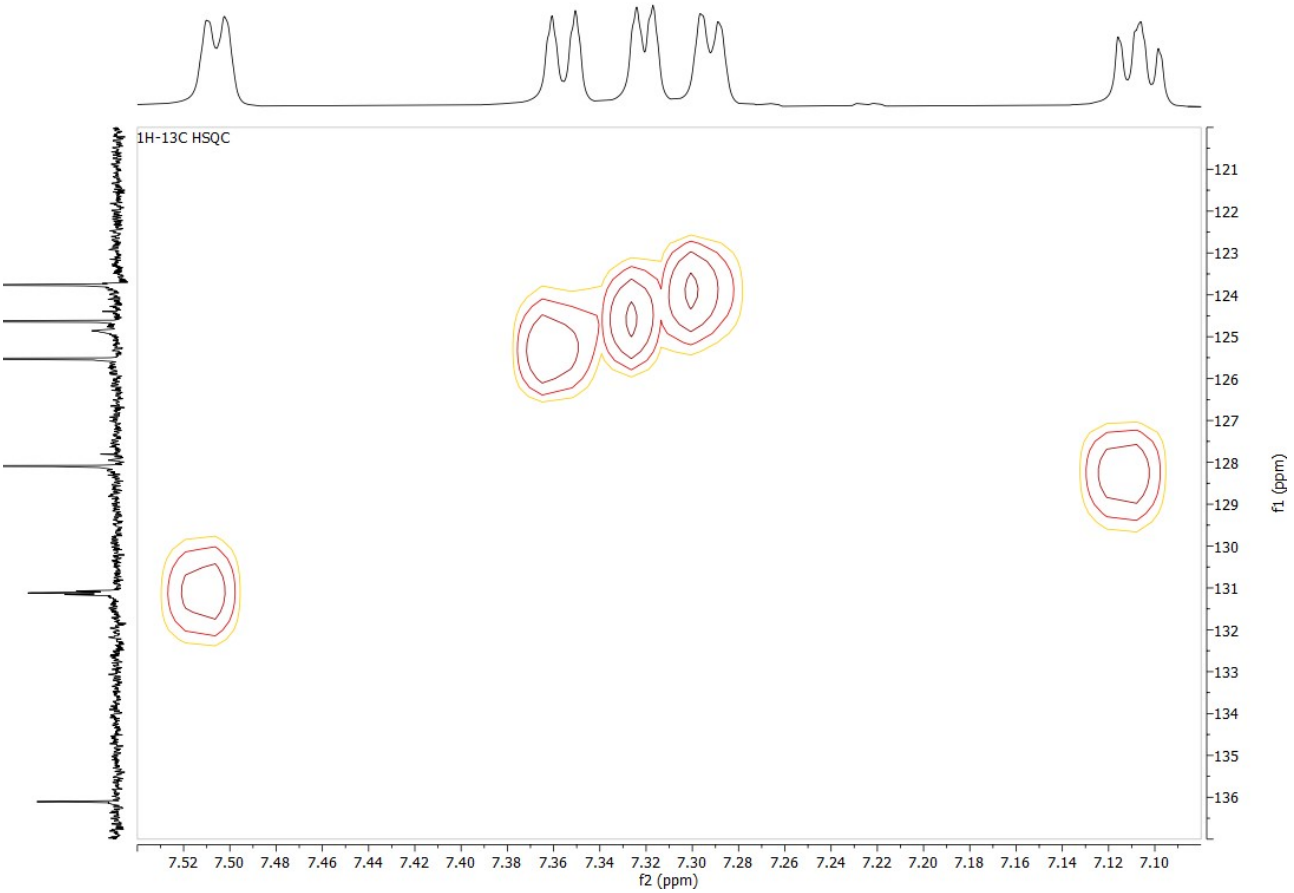


**Figure S22** $^{1}H$-$^{1}H$ COSY of 5-(pentafluorophenyl)-2,2'-bithiophene in $CD_2Cl_2$.

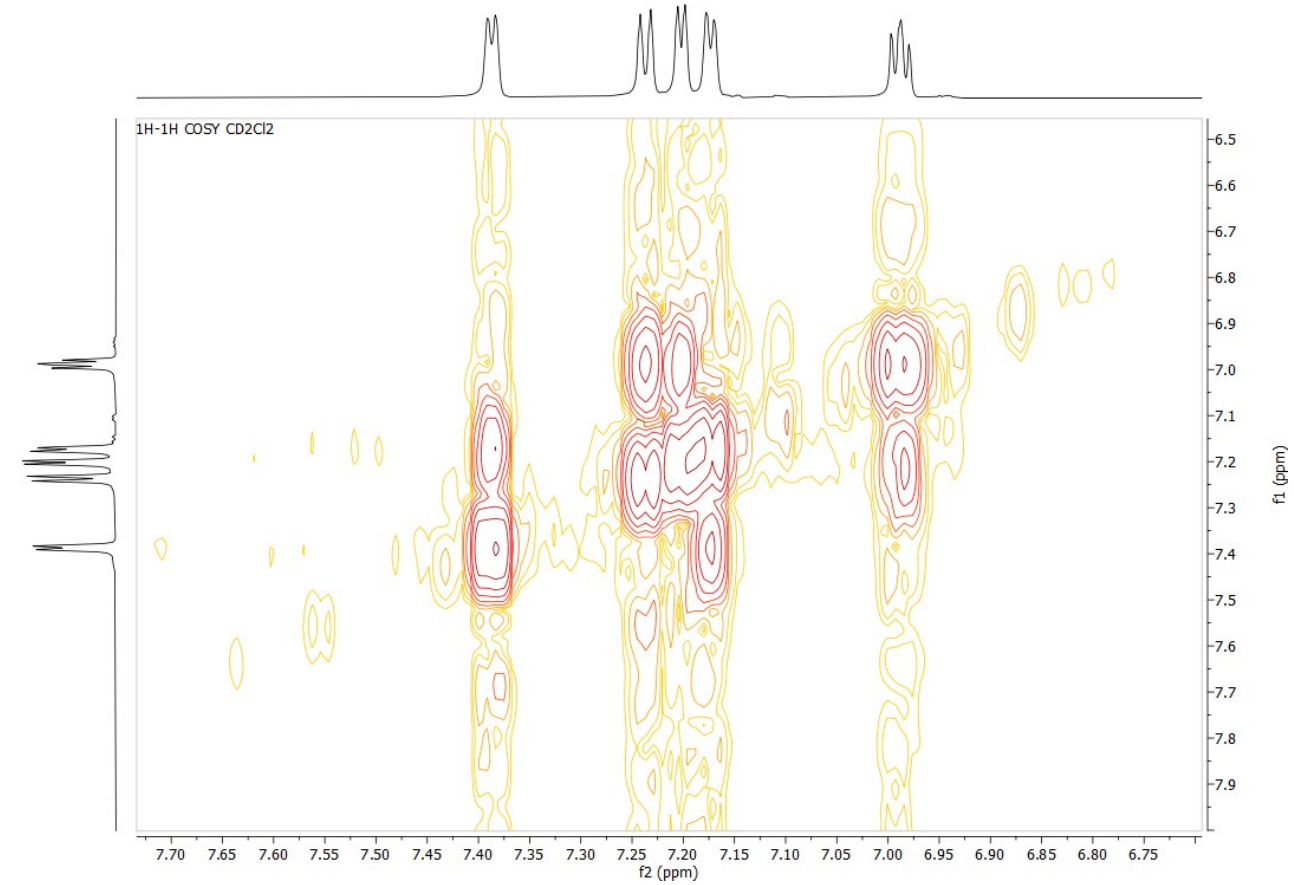


**Figure S23** $^{1}H$-$^{13}C$ HSQC of 5-(pentafluorophenyl)-2,2'-bithiophene in $CD_2Cl_2$.

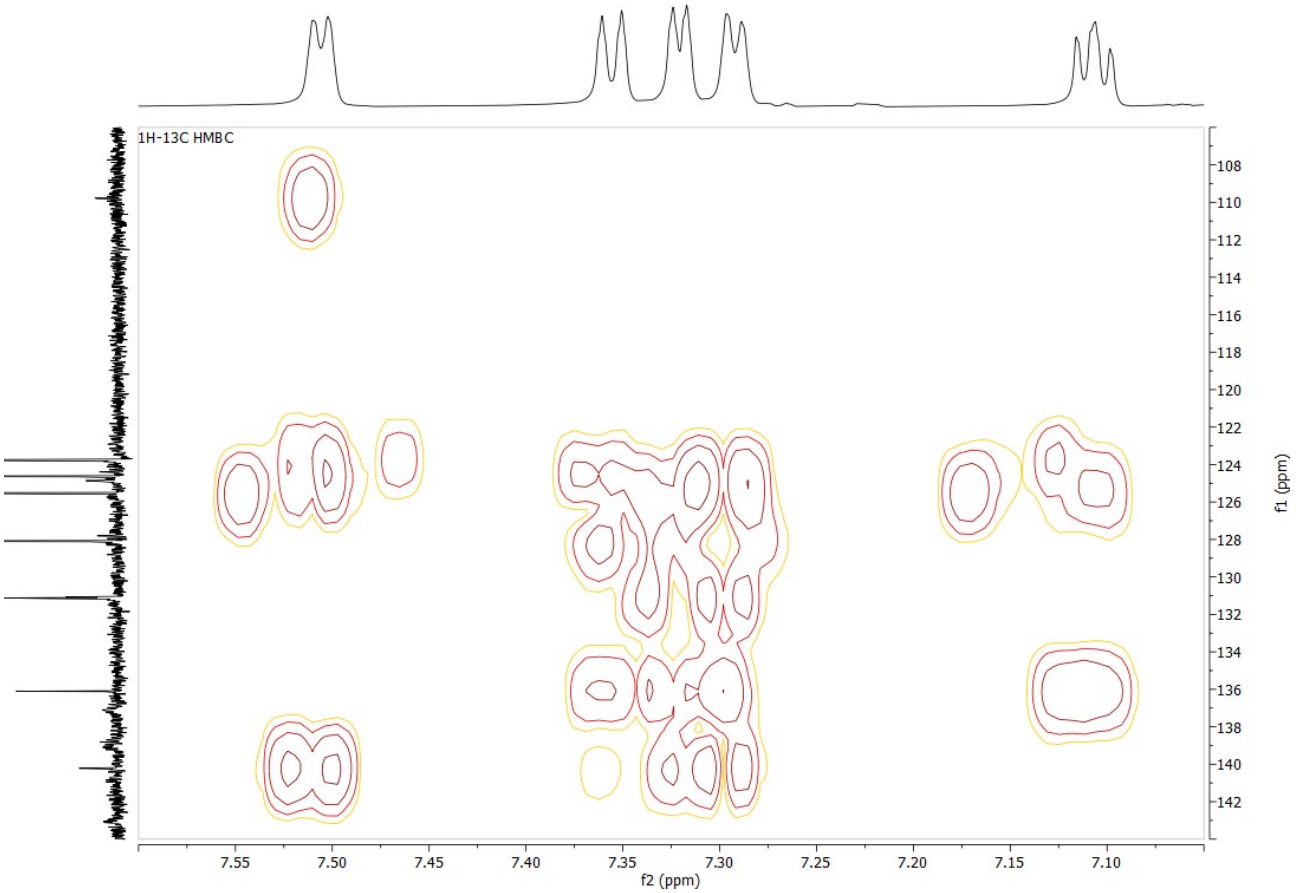


**Figure S24** $^{1}H$-$^{13}C$ HMBC of 5-(pentafluorophenyl)-2,2'-bithiophene in $CD_2Cl_2$.

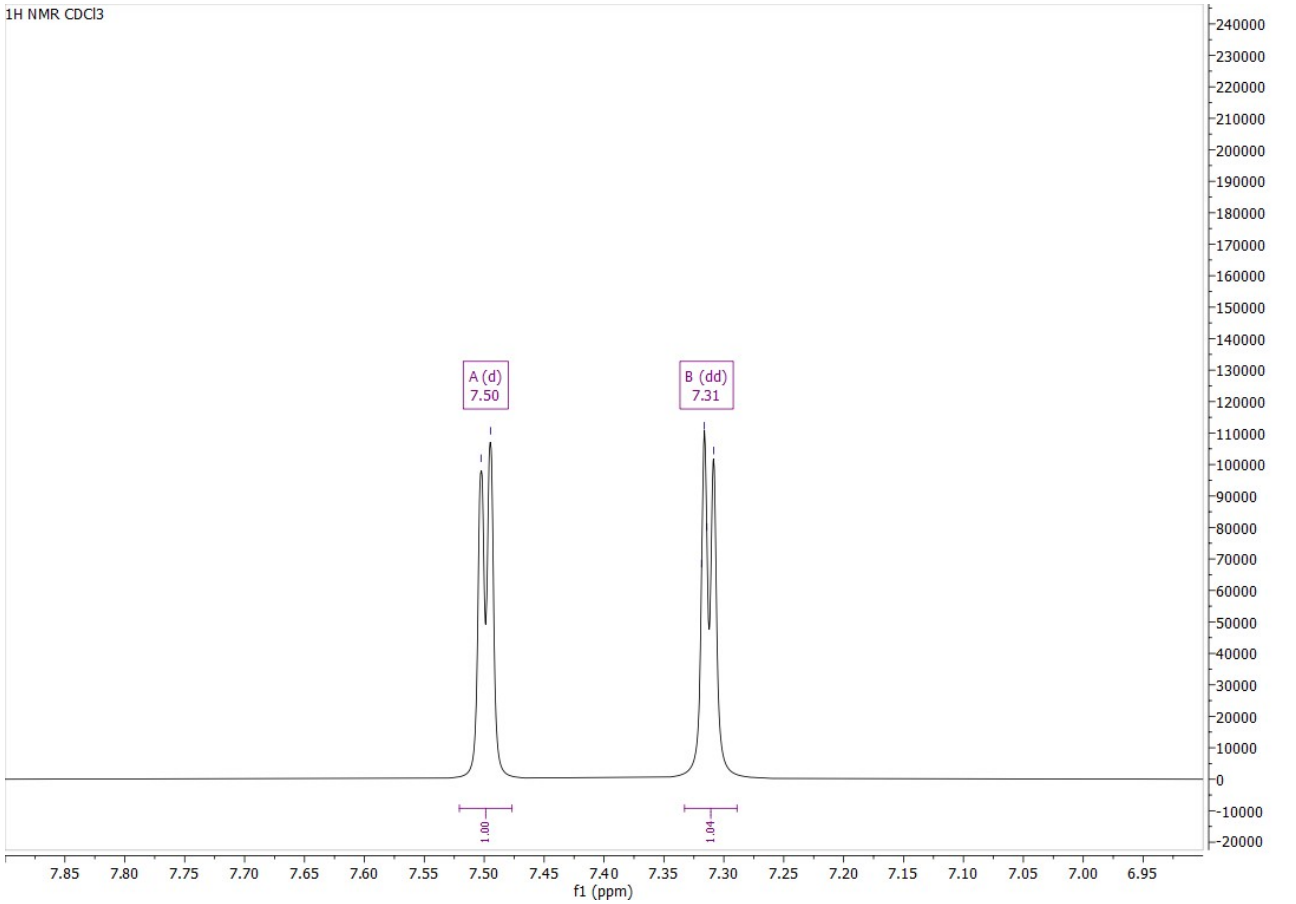


**Figure S25** $^{1}H$ NMR of 5,5'-bis(pentafluorophenyl)-2,2'-bithiophene in $CDCl_3$.

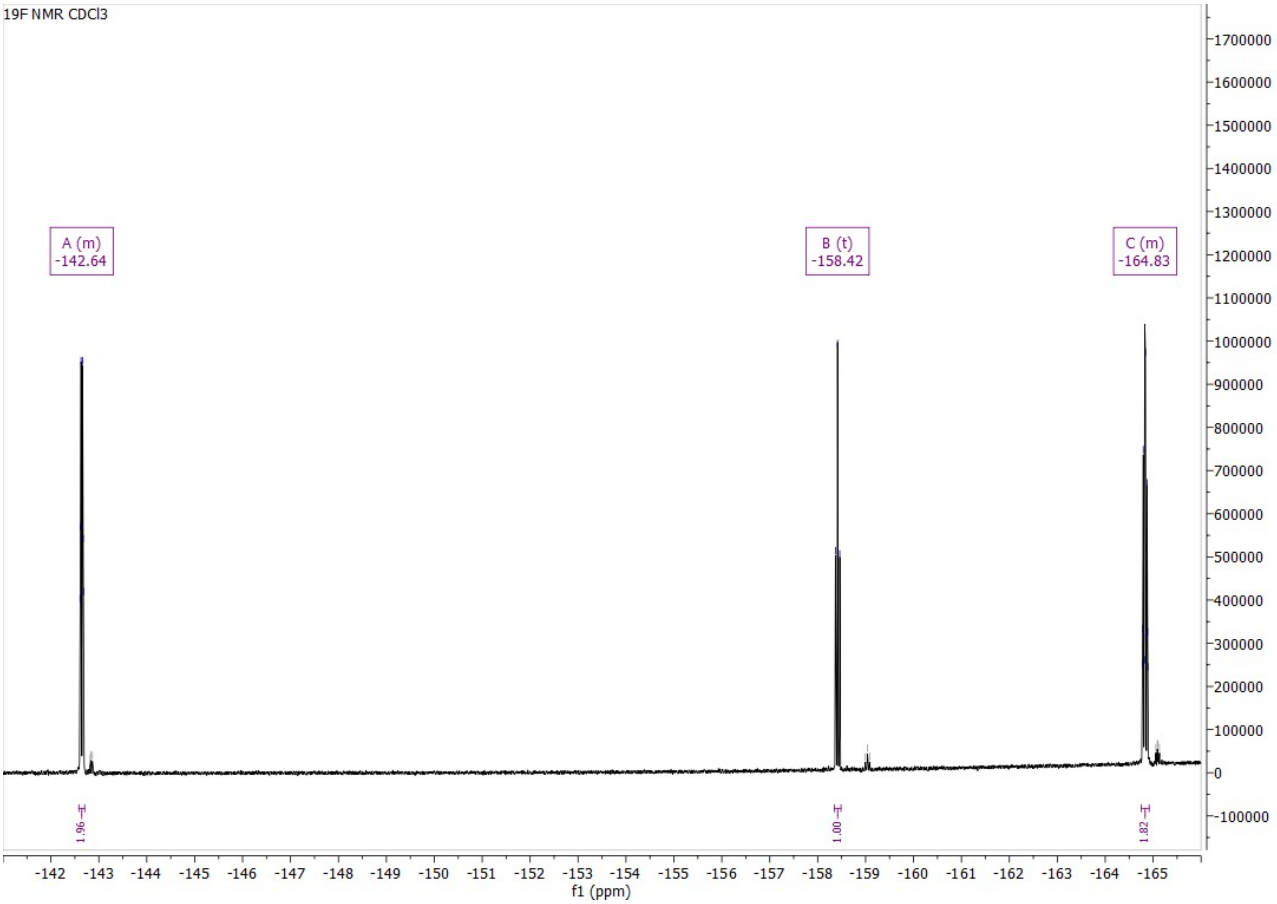


**Figure S26** $^{19}F$ NMR of 5,5'-bis(pentafluorophenyl)-2,2'-bithiophene in $CDCl_3$.

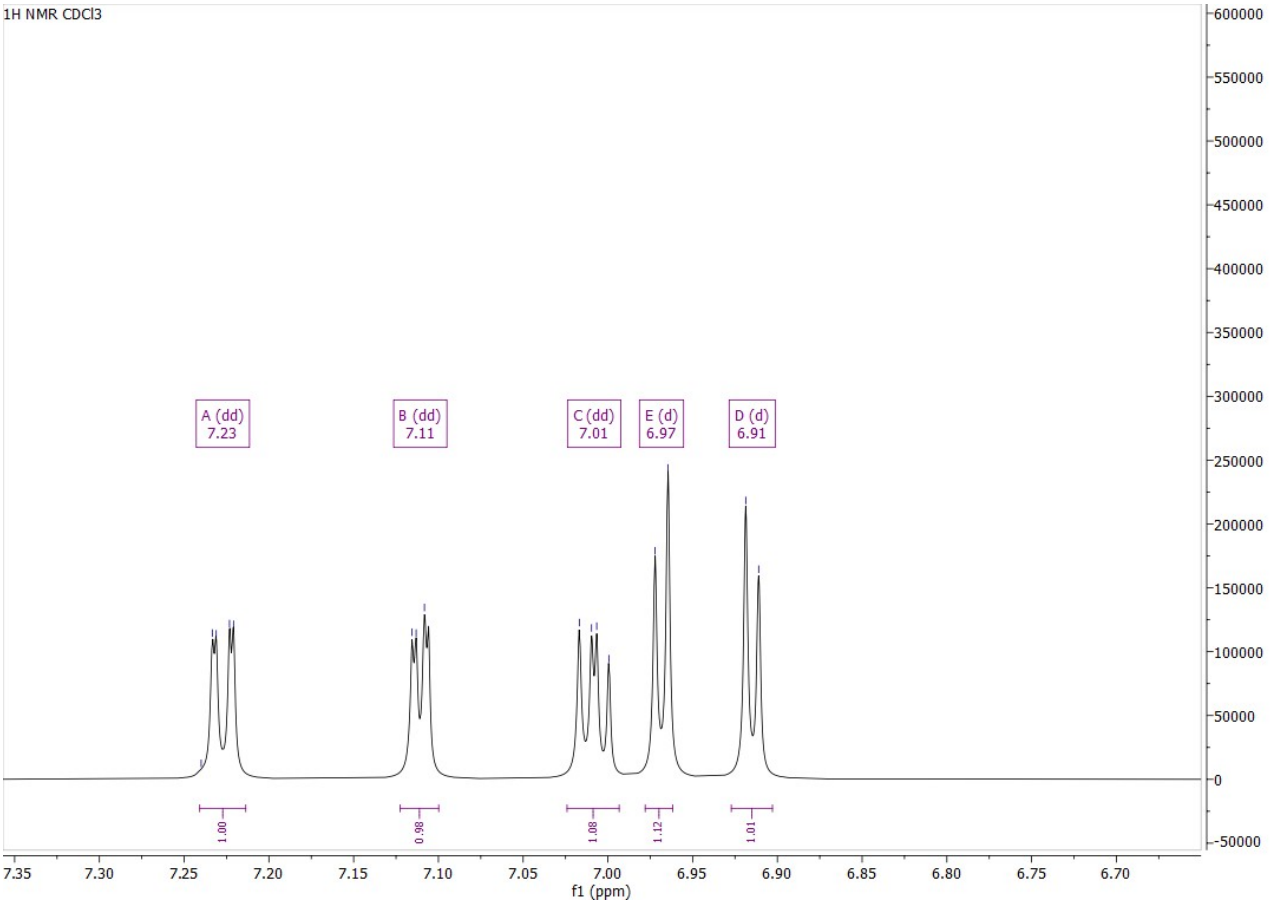


**Figure S27** $^{1}H$ NMR of 5-bromo-2,2'-bithiophene in $CDCl_3$.

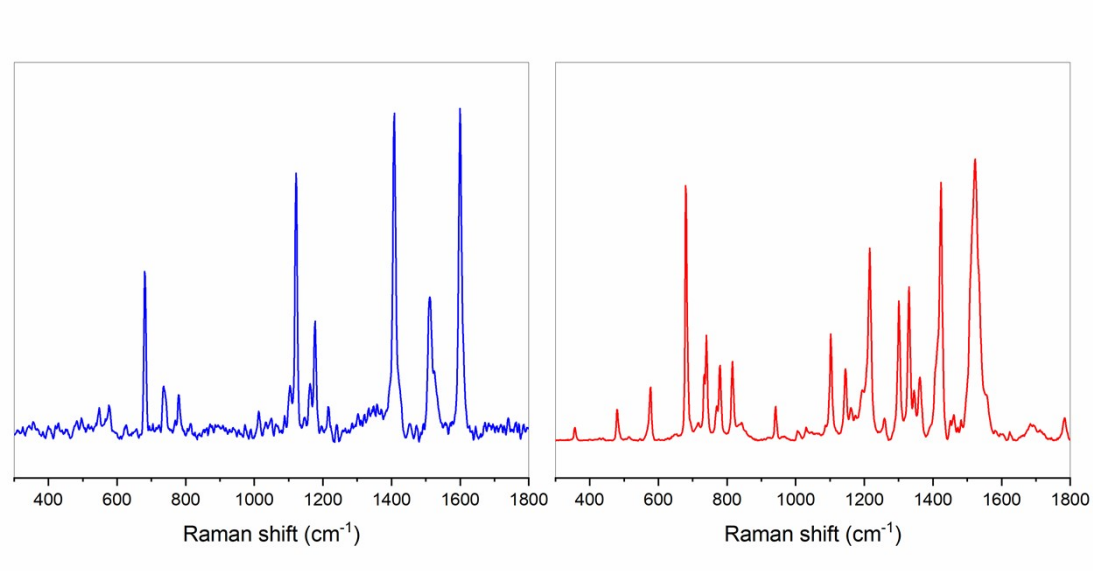


**Figure S28** Raman spectrum of $LuPc_2$.at 473 (left) and 633 nm (right), 0.5% edge of laser, 4 accumulations.

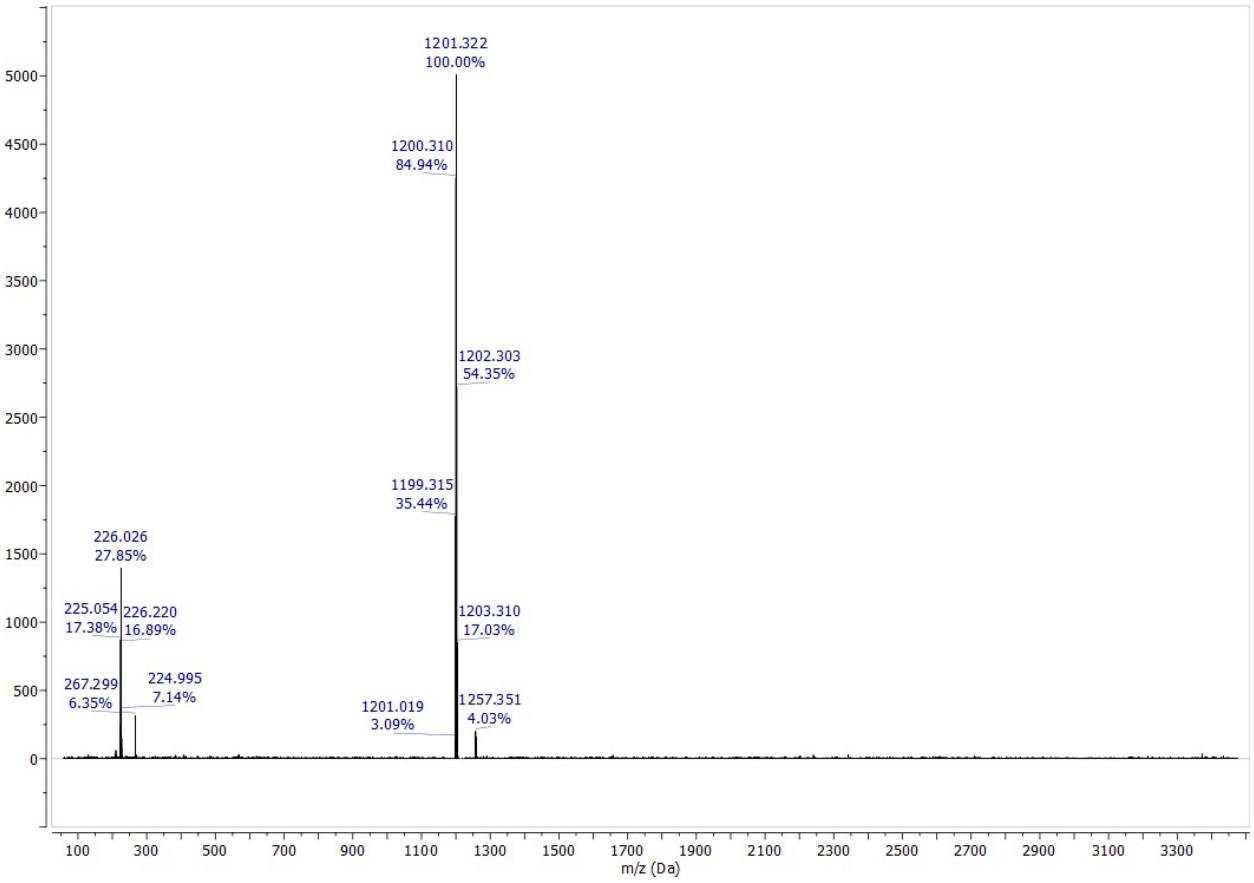


**Figure S29** MALDI-TOF mass spectra of $LuPc_2$ with dithranol (226 m/z) used as a matrix.

# References


1. A. Facchetti, M.-H. Yoon, C. L. Stern, H. E. Katz and T. J. Marks, *Angewandte Chemie*, 2003, **115**, 4030-4033.
2. Q. Niu, Y. Lu, H. Sun, X. Li and X. Tao, *Dyes and Pigments*, 2013, **97**, 184-197.
3. E. Ahmed, G. Ren, F. S. Kim, E. C. Hollenbeck and S. A. Jenekhe, *Chemistry of Materials*, 2011, **23**, 4563-4577.